International Journal of Nanoelectronics and Materials
IJNeaM
ISSN 198-5761 | E-ISSN 2232-1535

Study Influence of a Magnetic Field on Thin Film of (CdTe) Preparation via PLAL

Yamamah K. Abdalaah[a], Suaad S. Shaker[b,*], Olfat A. Mahmood[a]

[a]*University of Diyala, College of Science, Department of Physics, Diyala, Iraq*
[b]*University of Technology, Department of Applied Science, Baghdad, Iraq*
**Corresponding author. E-mail: suaad.salim@yahoo.com*

ABSTRACT

This work used pulsed laser ablation to influence a magnetic field to create CdTe (NPs) by using distilled water. According to X-ray diffraction results, the CdTe (NPs) product in a magnetic field is more crystalline. UV-Vis tests showed that CdTe (NPs) had an optical band gap shift from (1.75) eV to (2) eVEnergy-dispersive X-ray mapping confirmed the synthesis of CdTe (NPs) with a weight percentage ratio of 96% [Cd]/[Te]; the photoluminescence (PL) spectrum confirmed the emission of a solid and broad peak at (651.139). The current characteristics of the n-CdTe/p-SiHJ exhibit rectifying behavior when a magnetic field is applied., with the rectification factor rising from (48.351) to (62.105). The manufactured photodetector's spectral operating region was visible, with improved responsivity at 660 nm, increasing from 0.72 A/W to 0.84 A/W.

Keywords: *CdTe thin films, Laser ablation, Magnetic field*

1. INTRODUCTION

them apart from bulk materials, have drawn the attention of numerous researchers in recent times [1-4]. Because of their unique optical characteristics, CdTe nanoparticles (NPs), one of the II-VI semiconductor nanomaterials, have attracted the attention of many researchers [5–7].

CdTe, a highly absorbent P-type material, is ideal for thin-film solar cells due to its physiochemical characteristics. It includes an optical band gap that matches the AM1.5 spectrum at ambient temperature, resulting in an optical absorption coefficient of over 5×10^5 cm^{-1}. [8]. There are many methods to preparation nanoparticles Nps with different size and shapes such as pulsed laser deposition PLD, sel-gel and pulse laser ablation in liquid. the pulse laser ablation in liquid. Compared to traditional methods, this one offers numerous advantages, including the capacity to monitor the size and features of the generated nanoparticles and the assurance that they are free of contamination; it is also used to make different kinds of nanostructured materials [9]. The production process is also straightforward, inexpensive, and does not need pricey vacuum chambers. It is straightforward to manage the ejected nanostructures as a suspension or powder since they are entirely collected in solutions and form a colloidal solution. Additionally, this alternative physical nanofabrication technique offered new avenues for material processing based on the PLA of solids in different liquids to create various unique materials, including nano diamond [10,17]. Here in, we report on the preparation of CdTe (NPs) under the influence of a magnetic field by pulsed laser ablation (PLAL)methods. characteristics study and Fabrication of CdTe nanoparticles /Si photodetector as demonstrated.

2. EXPERIMENTAL PROCEDURE

Colloidal CdTe nanoparticles were produced employing a Q-switched Nd: YAG laser with a wavelength of 1064 nm and a pulse duration of 7 ns figure (1) a picture of the device used during work. High-purity CdTe powder pellets from Sigma Aldrich were pressed with a 1.2 cm radius hydraulic compressor to make colloidal CdTe nanoparticles. In first step: To prepare colloidal CdTe nanoparticles, the CdTe target was placed in the bottom of a glass vessel filled with distilled water and exposed to focused Nd: YAG laser pulses at a laser frequency of 100 pulses with a laser energy density of 5.3 J/cm2.To focus the laser light on the target, a converging lens with a 10 cm length of focus was used. And second steps of the same preparation conditions. An external magnetic field of 20 mT was produced using four tiny external neodymium magnets. A Tesla meter and Gauss were used to measure the magnetic field (NVIS 621). to investigate how the magnetic field affects the characteristics of colloidal CdTe NPs while they are being laser blasted. An X-ray diffractometer (Philips model X/Pert Pro), an ELICO, SL174, Spectrophotometer, and a UV-Vis double beam spectrophotometer (Shimadzu, 00,912,901-S) were used to measure the optical absorption of colloidal CdTe nanoparticles in order to investigate photoluminescences. Morphology, particle size, and chemical composition were estimated using A Field Emission Scanning Electron Microscope (FE-SEM) (MIRA3 model-TESCAN). The substrate was a 1 cm2 patch of mirror-like n-type silicon with an electrical resistance of 3–10 Ω cm. To remove the natural oxide, the silicon substrates were first cleaned and etched off the silicon surface using diluted HF. After that, the silicon substrate was once more cleaned for an average of fifteen minutes using an ultrasonic bath (Cerry PUL 125) and distilled water. Following cleaning, photodetectors were created by applying a room-temperature, thin layer of

CdTe (about 0.7 μm) on a silicon substrate using a spin coater (Holmarc HO-TH-05).. Ohmic contacts have been added to the CdTe film using the thermal resistive technique. The CdTe/n-Si heterojunction's current-voltage properties were measured at room temperature in the dark and under illumination. The photodetector's primary features, such as its spectral responsivity, were assessed using a calibrated electrometer, halogen lamp, DC power supply, and Jobin Yvon monochromator

Figure 1. Image of the device used in this work.

3. RESULT AND DISCUSSION

Figure 2 depicts the optical absorption of colloidal CdTe nanoparticles that were produced in both a 20 mT and no M-field. Smaller colloidal nanoparticles and a higher concentration of nanoparticles were made in the colloidal CdTe nanoparticles generated in a magnetic field during the ablation process.

In addition, their colour changed from brown to dark brown. It was supported by the photograph shown in Figure's inset Figure (2). Due to the increased nanoparticle concentration, CdTe NPs prepared with a magnetic field absorb lighter than those prepared without a magnetic field

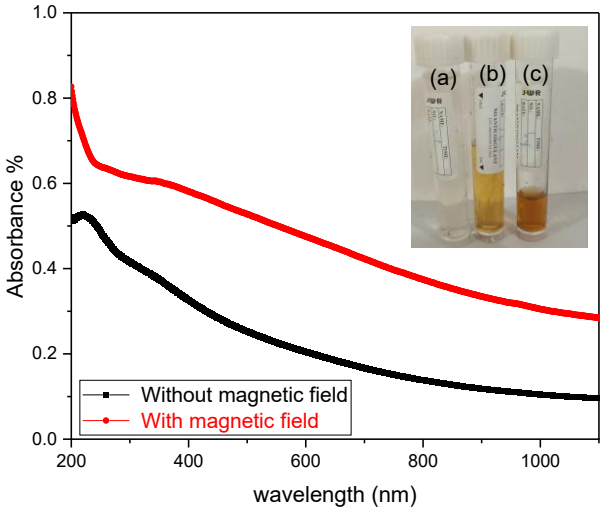

Figure 2. Optical absorption of CdTe colloid prepared without M-field(c) with 20 mT M-field. Inset is the photographs of colloids (a) water (b) without M-field(c) with 20 mT M-field.

As illustrated in Figure (3) for the CdTe sample prepared without M-field(c) with 20 mT M-field the energy band gap (Eg) of the allowed direct transmission was calculated using Tauc's equation [18,-21]:

$$\alpha h\nu = \beta (h\nu - E_g)^r \quad (1)$$

Where: α (absorption coefficient), hν (photon energy), β (band-tailing), r (It is a constant whose value depends on the type of electron transfer 1/2, 3/2, 2 and 3). The optical energy gap for CdTe NPs increased when a magnetic field was applied from (1.75) eV to (2.) eV. Due to the decrease in nanoparticle size [15,16The duration and density of the plasma are increased by magnetic confinement caused by an external magnetic field. As a result, more energy is transferred from the plasma to the liquid and target, increasing the amount of material that is ablated. [22, 23]

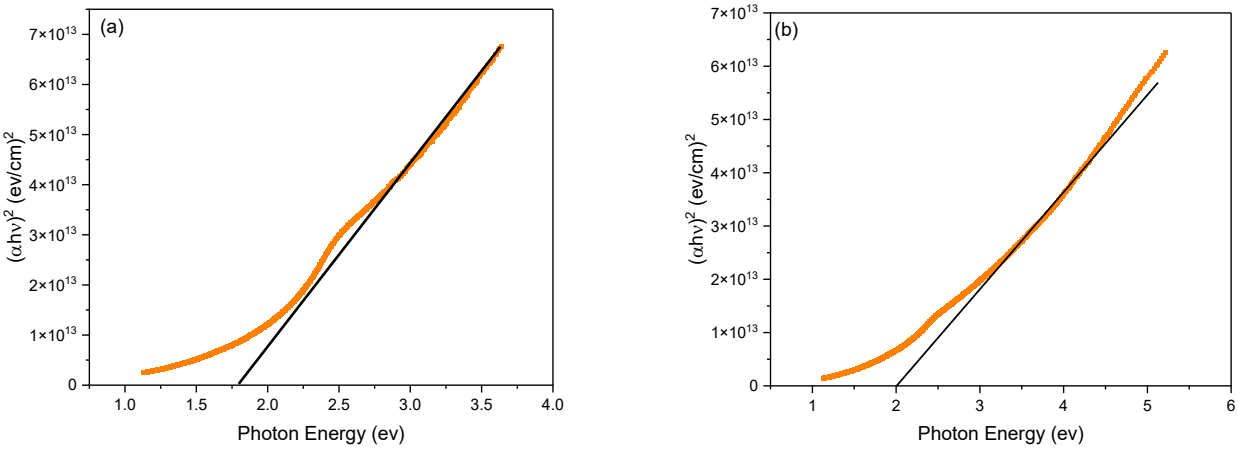

Figure 3. Direct optical energy gap for CdTe NPs prepared (a) without M-field B=0(b) with M-fieldB=20mT.

The PL emission spectra of CdTe NPs are illustrated in Figure (4), prepared without M-field B=0 and M-field B=20mT. The PL emission of a CdTe sample prepared with M-field B=20mT exhibits a single distinct emission peak with high intensity and a wide FWHM compared to the PL emission of a CdTe sample prepared without a magnetic field. CdTe prepared with a magnetic field was centered at (651.139) nm (1.904 eV), and the observed emission is displaced toward high energy or short wavelength. This results from the application of a magnetic field, which causes the size of the nanoparticles to decrease.

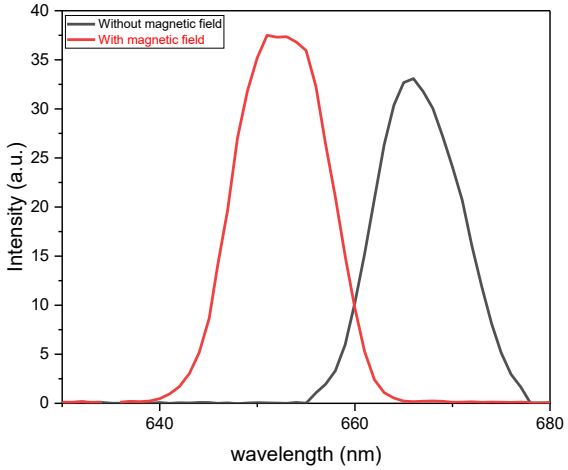

Figure 4. PL spectra of CdTe nanostructures colloidal synthesized without M-field B=0 and with M- field B=20mT.

The XRD pattern of CdTe nanoparticles generated at B = 0 and B = 20mT is displayed in Figure 5. Following the JCPDS card (no:15-0770).[17]. The XRD pattern of CdTe colloid Nanoparticles deposited on glass substrate showed diffraction peaks at 2θ = (23.7921°, 39.3074°, 46.4584°, 56.7745°, 62.4123°, 71.2342°, and 76.3345°) respectively, corresponding to the (111), (220), (311), (400), (331), (422), and (511) planes. The maximum intensity diffraction peak of the powder is also revealed by the XRD pattern at (2θ = 23.7921°). To index the diffraction data, the cubic phase and associated lattice constant value (a = 6.466 Å) were utilized [24The XRD pattern created using a magnetic field makes it evident that the CdTe peak's intensity increased. This outcome can be explained as improving the crystalline structure through increased crystallinity of the film material and reduced diffusion mobility of deposited atoms, which enhances the growth and nucleation properties [25]. The average size of crystallites from preferred orientation (111) was determined For CdTe Scherrer's formula produces (Dav) [26]:

$$D_{av} = (0.9\,\lambda) / (\beta \cos\theta) \qquad (2)$$

Where: β (full width at half maximum), θ (diffraction angle), and λ (wavelength). The results of the calculations indicated that the application of a magnetic field caused the concentration of CdTe NPs to decrease, resulting in a decrease in crystallite size from (40.7231) nm to (36.605) nm when compared to the crystallite size without the magnetic field. [25,27].

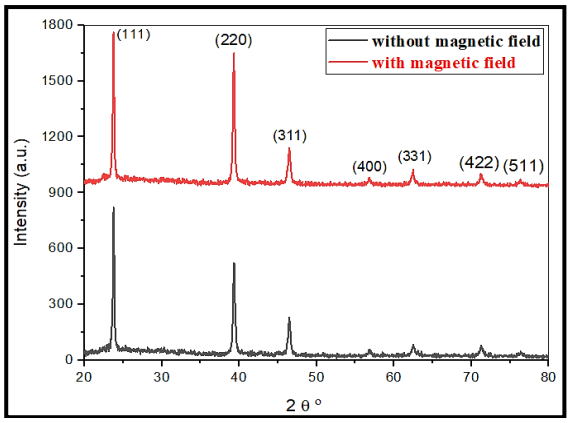

Figure 5. XRD patterns of CdTe nanostructures colloidal synthesized without M-field B=0 and with M- field B=20mT.

Figure (6b) exhibits CdTe nanoparticles generated in a magnetic field via laser ablation. as shown in the FESEM photos. When a magnetic field was absent, the film morphology in Figure (6a) was less homogeneous, dense, and compact. CdTe had an average particle size reduction from 26.17 nm to 20.92 nm. Figure 7 displays the EDS spectra of a CdTe NPs film that was produced magnetically. The elements Cd and Te are seen in these spectra, along with glass substrate-related peaks O, C, and S. The table shows the weight % ratio [Cd]/[Te] for CdTe NPs produced in a magnetic field, as measured by EDS analysis (1).

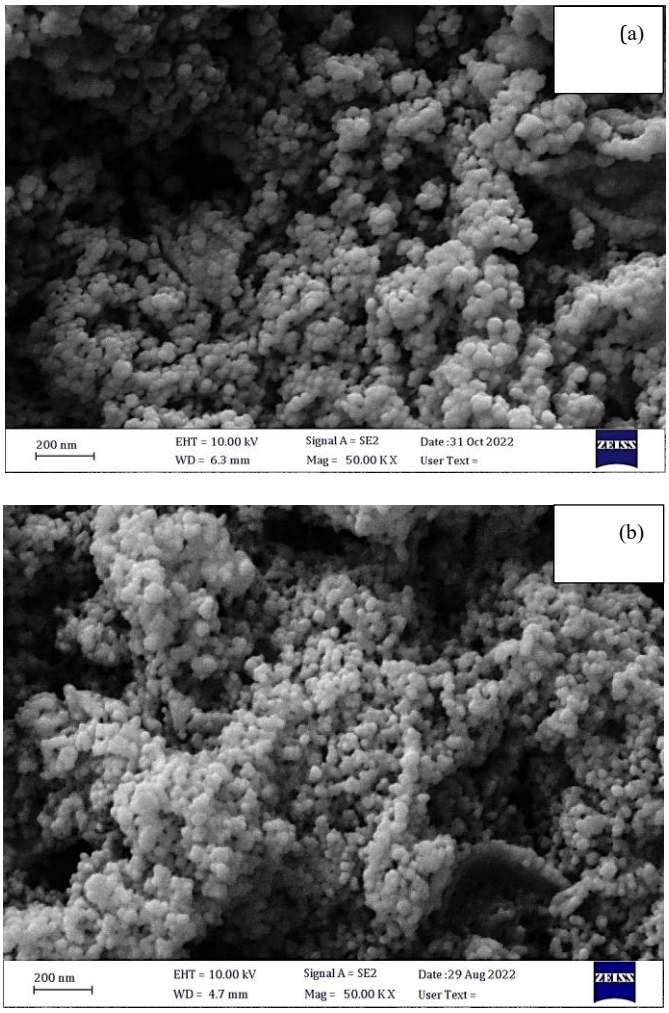

Figure 6. FESEM images of CdTe nanostructures colloidal synthesized without M-field B=0 and with M- field B=20mT.

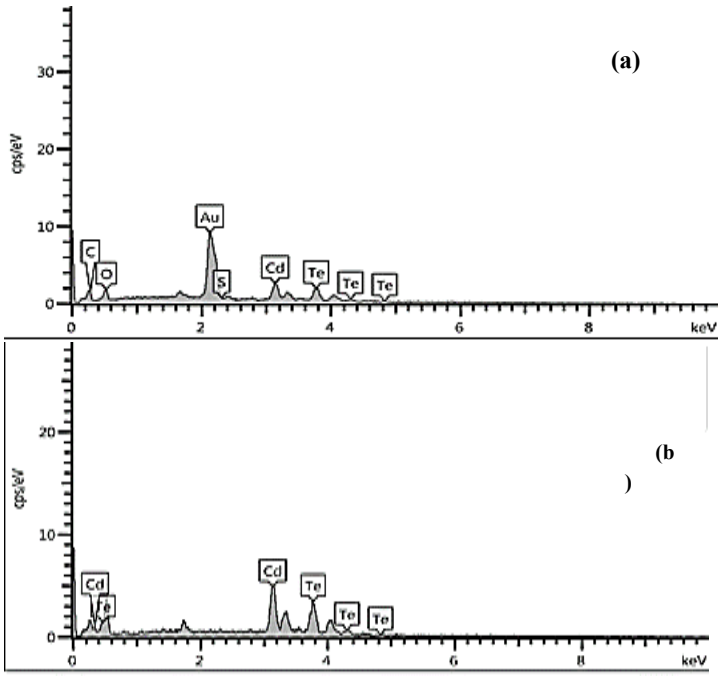

Figure 7. EDX spectra for CdTe NPs synthesised: (a) without M-field B=0 and (b) with M- field B=20mT.

Table 1 Elements and weight percentage for CdTe nanostructures colloidal synthesized without M-field B=0 and with M- field B=20mT

CdTe	Wt % (Cd)	Wt % (Te)	Ratio Cd:Te
With magnetic field	49.2	50.8	0.96
Without magnetic field	40.8	52.5	0.77

CdTe NPs film synthesized with a magnetic field was determined to be p-type based on Hall Effect measurements. When a magnetic field is applied, CdTe NPs' electrical mobility improves and their electrical resistance decreases, as the table illustrates. (2). The increase in electrical mobility and decrease in resistivity when applying amagnetic field can be attributed to improved crystallinity, which promotes nanoparticle alignment and crystallization, as well as enhanced Charge Carrier Separation. The magnetic field's alignment may allow for more efficient separation of electrons and holes, resulting in superior electrical characteristics. And Scattering at the grain boundary has been reduced. The magnetic field-induced alignment may reduce the number of grain boundaries or align them in a favorable direction, decreasing their adverse impact on electrical characteristics.

Table 2 Electrical mobility and resistivity of CdTe NPs

CdTe	Electrical Mobility ($cm^2 V^{-1} s^{-1}$) * 10^3	Electrical Resistivity (Ω cm)
Without magnetic field	8.97	3.98
With magnetic field	10.090	3.291

By applying a magnetic field, the dark I-V characteristics of the (p-CdTe/n-Si) heterojunction were studied, which extend the voltage range of -7.5 to +7.5 V, as shown in Figure 8. Because of the accelerated charge transfer and reduced resistance caused by the magnetic field, the heterojunction exhibits rectification features. The dark forward current for (p-CdTe/n-Si) increased from (440μA) to (590μA). For p-CdTe/n-Si HJ, the rectification factor increases from (48.351) to (62.105) when applying a magnetic field. This improvement is attributable to improved junction properties (a reduction in structural defects and surface states).

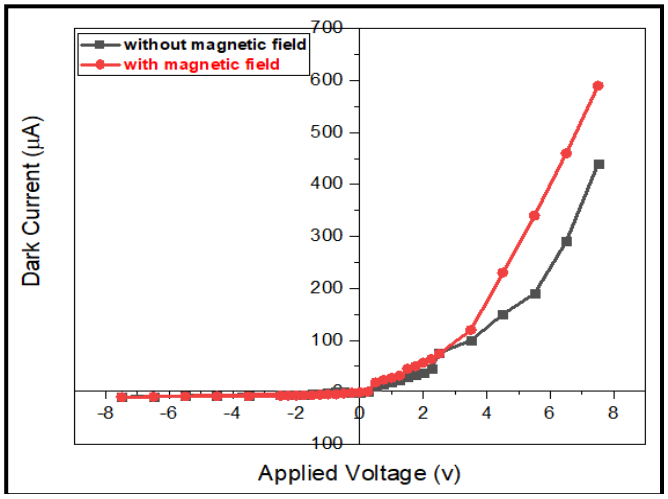

Figure 8. P-CdTe/n-Si heterojunction's dark I-V characteristic under forward and reverse bias.

Figure (9) depicts the I-V properties of the (p-CdTe/n-Si) heterojunctions in response to varying white light intensities and magnetic fields. When exposed to light, the photodetector's current increases due to the creation of an electron hole (e–h). As light intensity increases, photocurrent increases due to the growing number of photogenerated e–h couples. [28-34]. The photocurrent of the photodetector made in a magnetic field was higher than that of the photodetector made without one, as Figure (9b) illustrates. The increased surface area and light absorption could be the cause of this rise in photocurrent once a magnetic field is applied. When manufactured with a magnetic field at 7.5 V bias, The photocurrent to dark current ratio (Iph/Id) of the photodetector was 489.795 for (p-CdTe/n-Si). A decrease in particle size and an increase in the sensitive area are the reasons why applying the magnetic field increases the photodetector's photosensitivity. [33].

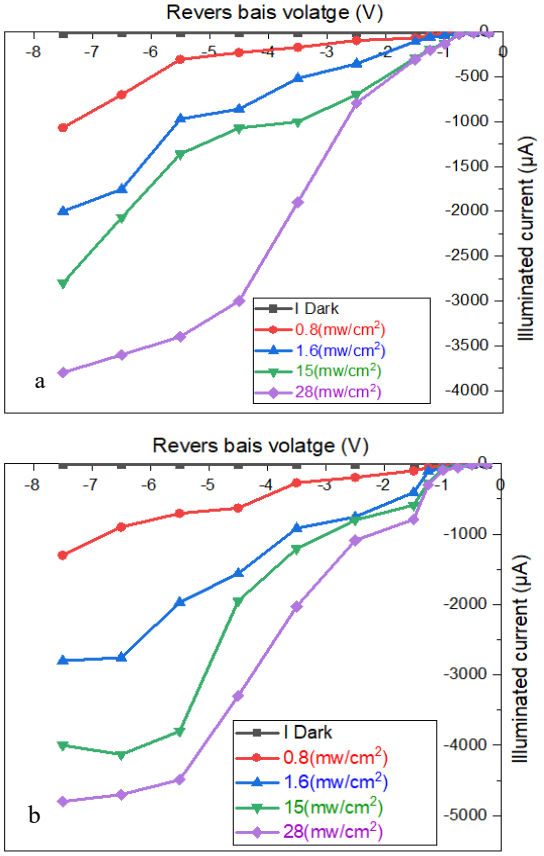

Figure 8. (I-V) Dark and illuminated characteristic of (p-CdTe/n-Si).

The spectral responsivity, which defines the ratio of output photocurrent to incident power, is a parameter used to measure the efficacy of any photodetectorSpectral responsivity measurement can be used to calculate the operating spectral region (Δλ), peak response (λP), and responsivity value. The spectral responsivity (Rλ) of p-CdTe/n-Si heterojunction was measured in the wavelength range of (360-910) nm with a bias of 0.65 V and calculated with the equation [35,36]:

$$R_\lambda = (I_{ph}/P_{in} \text{ or } V/P_{in}) \quad (3)$$

Figure 10 demonstrates how the application of a magnetic field affects the spectrum responsivity of a nanostructured (p-CdTe/n-Si) heterojunction photodetector. Two response peaks may be seen in photodetector responsivity data acquired both with and without a magnetic field. The first peak is located at 660 nm and is derived from the fundamental absorption of CdTe with responsivity (0.696 A/W). The second peak, on the other hand, is situated at 860 nm and is a part of the bulk silicon substrate's absorption edge. [16].

On the other hand, when a magnetic field is applied, the responsivity increases from 0.72 A/W to 0.84 A/W, with the first peak occurring at 660 nm. Additionally, the second peak, which has a responsivity of 1.2 A/W, can also be found at 860 nm.

REFERENCE

[1] N. G. Semaltianos, S. Logothetidis, S.Romani , (2008). II–VI semiconductor nanoparticles synthesized by laser ablation. Journal of Applied Physics A, 94(3), 641–647.

[2] S. A. Lourenco, R. S. Silva, A. C. Rabelo, G. D. A. Rocha, &N. O. Danta, (2017). Optical Properties of Semiconductor Nanocrystals into the Glass and Colloidal Environments for New Technological Applications". Recent Advances in Complex Functional Materials. Springer, Cham. 155-175.

[3] A. I. Savchuk, A. Perrone, A. Lorusso, I.D. Stolyarchuk, O. A. Savchuk, &O. A. Shporta, (2014). ZnMnO diluted magnetic semiconductor nanoparticles: Synthesis by laser ablation in liquids, optical and magneto-optical properties." Applied Surface Science, 302: 205-208.

[4] D. A. Goncharova, I. N. Lapin, and V. Svetlichnyi, (2015). Synthesis of CdS nanoparticles by laser ablation of metallic cadmium target in presence different precursors." Advanced Materials Research. Trans Tech Publications. 1085(182-186).

[5] S. Chandra, S. T. Sundari, G. Raghavan and A. K Tyagi, (2003). Optical properties of CdTe nanoparticle thin films studied by spectroscopic ellipsometry". J. Phys. D: Appl. Phys, 36, (2121-2129).

[6] Z. Tang, Z. Zhang, Y. Wang, S. C. Glotzer, N. A. Kotov (2006) .Self Assembly of CdTe Nanocrystals into Free-Floating Sheets". Science. 314, 274-278.

[7] S. Wang, Y. Li, Y. Yang, Y. Song, & C. Zhang, (2009). Characterization and photoluminescence studies of CdTe nanoparticles before and after transfer from liquid phase to polystyrene". Bulletin of Materials Science, 32.5: 487.

[8] K. S. Khashan, G. M. Sulaiman, A. H. Hamad, F.A. Abdulameer, & A. Hadi, (2017). Generation of NiO nanoparticles via pulsed laser ablation in deionised water and their antibacterial activity. Applied Physics A, 123(3), 190.

[9] J. B. Wang, C. Y. Zhong, X. L. Zhong, G. W. Yang, (2002). Cubic and hexagonal structures of diamond nanocrystals formed upon pulsed laser induced liquid–solid interfacial reaction. Chemical Physics Letters, 361(1–2), 86–90.

[10] L. Yang, P. W. May, Y. L. Smith, J. A. Rosser, K. N., (2007). Growth of diamond nanocrystals by pulsed laser ablation of graphite in liquid". Diamond and Related Materials, 16(4–7), 725–729.

[11] S. S. Shaker, R. A. Ismail & B. K. Mohammed, (2023). Preparation of Graphene Oxide@ZrO2 Core/Shell Nanoparticles by Two-Step Laser Ablation in Liquid Towards a High-Performance Silicon-Based Heterojunction Photodetector. Springer, 5791–5802.

[12] K. H. Jawad, B. A. Hasoon, R. A. Ismail, S. S. Shaker , (2022).Preparation of copper oxide nanosheets by pulsed laser ablation in liquid for anticancer, antioxidant, and antibacterial activities. Indian Chemical Society. 99(11).

[13] S. S. Shaker, R. A. Ismail, D. S. Ahmed, (2022). High-Responsivity Heterojunction Photodetector Based on Bi2O3-Decorated MWCNTs Nanostructure Grown on Silicon via Laser Ablation in Liquid. Journal of Inorganic and Organometallic Polymers and Materials, 32(5):1-8.

[14] R. A. Ismail, S. S. Shaker & S.F. Abdulmuneem, (2022). Preparation of nanostructured PbI2/Si photodetector by magnetic field-assisted laser ablation in liquid. Silicon, 14(10291–10300).

[15] S. S. Shaker, R. A. Ismail, D. S. Ahmed, (2022). Preparation of Bismuth Oxide Nanoplatelets/Si Photodetector by Laser Ablation in Liquid Under Effect of an External Magnetic Field. Silicon ,14(1):1-7.

[16] Y. K. Abdalaah, O. A. Mahmood, S. S. Shaker, & R. A. Ismail, (2024). Preparation of a nanostructured CdTe@ CdS core–shell/Si photodetector by two-step laser ablation in liquid. Journal of Optics, 1-12.

[17] A. V. Kabashina, & M. Meunier, (2003). Synthesis of colloidal nanoparticles during femtosecond laser ablation of gold in water", Journal of Applied Physics, 94(15).

[18] A. A. Najim, S. S. Shaker & M. A. H. Muhi, (2017) . Room Temperature NO2 Gas Sensor Based on SnO2-WO3 Thin Films. Plasmonics ,12:1051–1055.

[19] M. M. Ismail1, S.S. Shaker & R. A. Kamil, (2023). Influence of Pulse Laser Energy on Structural and Magnetic Properties of CoFe2O4 and CoLa0.01Fe1.99O4 Thin Films. Journal of Solid State Science and Technology, 12 (3).

[20] R. A. Kamil, M. M Ismail, S. S. Shaker, (2023). Characterization of CoLaxFe2−xO4 Spinel Thin Films Using Pulse Laser Deposition. Journal of Superconductivity and Novel Magnetism 35(5):1-9.
[21] A. J. Haider, A. J. Mohammed, S. S. Shaker, K. Z. Yahya, M. J. Haider, (2017). Sensing Characteristics of Nanostructured SnO 2 Thin Films as Glucose Sensor. Energy Procedia. 119, 473-481.
[22] C. S. Ferekides, D. Marinskiy, V. Viswanathan, B. Tetali, V. Palekis, P. Selvaraj& D. L. Morel, (2000). High efficiency CSS CdTe solar cells. Thin Solid Films, 361, 520-526.
[23] C. Potamialis, (2019). Process sensitivities and interface optimisation of CdTe solar cells deposited by close-space sublimation" (Doctoral dissertation, Loughborough University).
[24] R. S. Alnaily, M. L. Sheqnab, (2019). Study the optical and structure properties of CdTe nanoparticles prepared by pulsing laser ablation in distilled water", JOURNAL OF KUFA–PHYSICS, 11(1).
[25] N. Wakiya, T. Kawaguchi, N. Sakamoto, H. Das, K. Shinozaki, H. Suzuki, (2017). Progress and impact of magnetic field application during pulsed laser deposition (PLD) on ceramic thin films", Journal of the Ceramic Society of Japan, 125(12) 856-921.
[26] R. Ismail, A. M. Mousa, S. S. Shaker, (2019). Pulsed laser deposition of nanostructured MgO film: Effect of laser fluence on the structural and optical properties. Materials Research Express. 6(7).
[27] F. Hubenthal, T. Ziegler, C. Hendrich, M. Alschinger, and F. Trager, (2005). Tuning the surface plasmon resonance by preparation of gold-core/silver-shell and alloy nanoparticles, European Physical Journal D, Vol. 34, pp. 165-168.
[28] N. Z. Abed, R. A. Ismail & S. S. Shaker. (2024). Role of substrate temperature on the performance of BaTiO3/Si photodetector prepared by pulsed laser deposition. Scientifc Reports, 14:4531.
[29] R. A. Ismail, A. D. Faisal, S. S. Shaker,(2022).Preparation of ZnS-decorated MWCNTs/p-Si hybrid photodetector by pulsed laser deposition. Optical Materials. 133, 112998.
[30] R. Ismail, N. Hasan, S. S. Shaker, (2021). Preparation of Bi2Sr2CaCu2Ox Thin Film by Pulsed Laser Deposition for Optoelectronic Devices Application. Silicon 14(2A):1-9.
[31] S. S. Shaker, S. I. Younis, J. M. Moosa, R. A. Ismail, (2021). Pulsed laser deposition of nanostructured HgI2 on Si substrate for photodetector application. Materials Science in Semiconductor Processing, 135, 106106.
[32] R. A. Ismail, S. S. Shaker, A. M. Mousa, (2021). Study the optoelectronic properties of PbI2 nanorods/Si photodetector prepared by magnetic field-assisted laser deposition route. Optics & Laser Technology. 140, 107042.
[33] R. Ismail, A. M. Mousa, S. S. Shaker, (2019). Improved growth conditions of pulsed laser-deposited PbI2 nanostructure film: towards high- photosensitivity PbI2/CNTs/Si photodetectors. Journal of Materials Science: Materials in Electronics 30(23).
[34] R. Ismail, A. M. Mousa, S. S. Shaker, (2019). Visible-enhanced silver-doped PbI2 nanostructure/Si heterojunction photodetector: effect of doping concentration on photodetector parameters. Optical and Quantum Electronics, 51(11).
[35] R. Ismail, A. M. Mousa, S. S. Shaker, (2020). Preparation of visible-enhanced PbI2/MgO/ Si heterojunction photodetector. Optik, 202, 163585.
[36] R. Ismail, A. M. Mousa, S. S. Shaker, (2019). Effect of substrate temperature on the characteristic of p-PbI2 /n-Si heterojunction grown by pulsed laser deposition technique. Materials Science in Semiconductor Processing. 99:165-174.